Advancing the Development of Wind Energy Across Canada

Story Page 6

Sulphur Diffusion in β-NiAl and Effect of Pt additive: An ab inito Study

Page 10

WINTER 2013/2014 hiver

CSME Executive & Staff/Officiers et personnel SCGM

BOARD OF DIRECTORS / CONSEIL D'ADMINISTRATION

President / Président	Christine Wu, FCSME	cwu@cc.manitoba.ca
Sr. Vice President / Premier vice Président	Ali Dolatabadi, FCSME	Ali.Dolatabadi@concordia.ca
Past President / Président sortant	Kamran Behdinan, FCSME	behdinan@mie.utoronto.ca
Honorary Treasurer / Trésorier honoraire	John Hayes, FCSME	jhayes@mae.carleton.ca
Honorary Secretary / Secrétaire honoraire	David Weaver, FCSME	weaverds@mcmaster.ca

REGIONAL VICE PRESIDENTS / VICE-PRÉSIDENTS RÉGIONAUX

Western Region / Région de l'Ouest	Homayoun Najjaran, MCSME	Homayoun.Najjaran@ubc.ca
Ontario Region / Région de l'Ontario	Payam Rahimi, MCSME	prahimi@ualberta.ca
Quebec Region / Région du Québec	Pierre Gauthier, MCSME	gauthier@encs.concordia.ca
Atlantic Region / Région de l'Atlantique	Dominic Groulx, MCSME	dominic.groulx@dal.ca

STANDING COMMITTEES / COMITÉS PERMANENTS

Membership	David Naylor, FCSME	dnaylor@ryerson.ca
Student Affairs / Affaire étudiantes	Sushanta Mitra, FCSME	sushanta.mitra@ualberta.ca
Student Design Competition / Concours de design des étudiants		
Student Paper Competiton/ Concours de publication des étudiants		

TECHNICAL COMMITTEES / COMITÉS TECHNIQUES

Codes and Standards / Codes et normes		
Thermo-Fluids Engineering/ Génie thermique		
Materials Technology / Technologie des matériaux	Chul Park, FCSME	park@mie.utoronto.ca
Environmental Engineering / Génie de l'environnement	Horia Hangan, MCSME	hmh@blwtl.uwo.ca
Transportation Systems / Systèmes de transport	Ebrahim Esmailzadeh, FCSME	Ebrahim.Esmailzadeh@uoit.ca
Manufacturing & Robotics / Fabrication et robotique	Jack Jeswiet, MCSME	jeswiet@me.queensu.ca
Engineering Analysis & Design / Conception et analyse en ingénierie	II Yong Kim, MCSME	iykim@me.queensu.ca
Mechatronics and Mems / Mécatronique	Jeff Piepper, FCSME	pieper@ucalgary.ca
Biomechanics/Biomécanique	Edward Park, MCSME	ejpark@me.uvic.ca
Advanced Energy Systems	Xianguo Li, FCSME	x6li@uwaterloo.ca
MEMS/Nanotechnology	Nezih Mrad, MCSME	nezih.mrad@nrc-cnrc.ca

PUBLICATIONS

Editor, Transactions / Rédacteur, Transactions	Paul Zsombor-Murray, FCSME	paul@cim.mcgill.ca
Managing Editor / Rédacteur administrateur	Ilian Bonev, MCSME	ilian.bonev@etsmtl.ca
Technical Editor, Bulletin / Rédacteur technique, Bulletin	Kamran Siddiqui, FCSME	ksiddiqui@eng.uwo.ca
Editor, Bulletin / Rédacteur, Bulletin	Xiaodong Wang, FCSME	xiaodong.wang@ualberta.ca

SPECIAL COMMITTEES / COMITÉS SPÉCIAUX

History Committee / Comité de l'histoire	Hugh Mcqueen, FCSME	mcqueen@encs.concordia.ca
Corporate Membership / Membres corporatifs	Mike Clark, MCSME	mike.clark@litens.com
Honors and Awards	Kamran Behdinan, FCSME	behdinan@mie.utoronto.ca

CSME OFFICE / BUREAU SCGM

Executive Director /Administrateur	John Plant, Ph.D	jplant1@cogeco.ca

CSME/SCGM

1295 Highway 2 East
Kingston, ON K7L 4V1

Phone / Téléphone (613) 547-5989   Fax / Télécopieur (613) 547-0195   Email csme@cogeco.ca   www.csme-scgm.ca

Christine Wu, Ph.D., P.Eng., FCSME

President's Message

While over 6,000 athletes from 85 countries gather for the 2014 Winter Olympics in Sochi, the level of competition and sportsmanship are truly breathtaking. What impressed me as much as the athletic performance is to see the engineering behind the Winter Olympics. How can engineers build faster and safer bobsleds? How can engineers design competition suits to improve aerodynamics by reducing friction and drag? How can engineers make perfect ice for speed skaters? It is equally impressive to see how the athlete's movements inspire the robotic design. It is an exciting time not only for athletes but also for engineers.

2014 is also an exciting year for CSME. I would like to take this opportunity to congratulate Dr. Greg F. Naterer, Dean of Faculty of Engineering and Applied Science from Memorial University for receiving the Julian C. Smith Medal. The Julian C. Smith Medal is given by EIC to the recipient for Achievement in the Development of Canada. I would also like to congratulate Dr. Sushanta Mitra, Professor of the Department of Mechanical Engineering from University of Alberta and Dr. Nasser Ashgriz, Professor of the Department of Mechanical and Industrial Engineering from University of Toronto, who are elected as EIC Fellows.

I look forward to seeing you at the upcoming CSME International Congress 2014, which will be held at University of Toronto. The Congress Chair, Dr. Jean Zu, her Co-Chair, Dr. Kamran Behdinan and the organizing committee have invited world-class keynote speakers, attracted 4 concurrent conferences and 14 special symposiums encompassing all aspects of Mechanical Engineering. This is the first time that CSME and CFDSC organize their flagship conferences together. The bi-annual CEME Undergraduate Design Competition and CSME Graduate Students Research Paper Competition will showcase the outstanding achievements of undergraduate and graduate students from the Canadian Universities. The CSME honors, awards and fellowships will be announced at the conference banquette. The awards for the winning teams in the CSME Design Engineering competition and for the best paper awards will also be announced at the same banquet.

This is a great time to get involved and stay involved in CSME. Let's work together toward to building engineering in Canada and around the world.

Christine Q. Wu, Ph.D., P.Eng., FCSME
Professor and NSERC Industrial Research Chair
Department of Mechanical and Manufacturing Engineering
University of Manitoba

Plus de 6 000 athlètes de 85 pays se sont réuni pour les jeux olympiques d'hiver 2014 à Sotchi. Le niveau de compétition et l'esprit sportif ont était tout simplement à couper le souffle. Ce qui m'a impressionné autant que la performance des athlètes c'est de voir le génie derrière les jeux olympiques d'hiver. Comment font les ingénieurs pour construire un bobsleigh plus rapides et plus sécuritaire? Comment font les ingénieurs pour concevoir les costumes pour améliorer l'aérodynamisme en réduisant la friction et la trainée? Comment font les ingénieurs pour faire une glace parfaite pour les patineurs de vitesse? Il est tout aussi impressionnant de voir comment la mobilité de l'athlète inspire la conception robotique. Les jeux olympiques sont des évènements inspirant non seulement pour les athlètes, mais aussi pour les ingénieurs.

L'année 2014 est également une année passionnante pour la SCGM. Je veux profiter de cette occasion pour féliciter le Greg F. Naterer, doyen de la faculté de génie et sciences appliquées de l'Université Memorial pour l'obtention de la médaille Julian C. Smith. La médaille Julian C. Smith est donnée par l'institut canadien des ingénieurs pour réussite dans le développement du Canada. Je voudrais également féliciter Sushanta Mitra, professeur du département de génie mécanique de l'Université de l'Alberta et Nasser Ashgriz, professeur du département de mécanique et génie industriel de l'Université de Toronto, qui sont attribué le titre de « Fellow » par l'institut canadien des ingénieurs.

J'ai également hâte de vous voir au prochain congrès international de la SCGM, qui aura lieu à l'Université de Toronto en 2014. La présidente du congrès, Jean Zu, son co-président, Kamran Behdinan et le comité organisateur ont invités des conférenciers de renommée internationale, ont attiré 4 conférences simultanées et 14 colloques spéciales englobant tous les aspects du génie mécanique. C'est la première fois que SCGM et SCCFD organisent leurs conférences phares ensemble. La compétition biannuelle de conception pour les étudiants en génie CEME et la compétition aux cycles supérieurs de travaux de recherche mettra en valeur les réalisations de tous les étudiants en génie mécanique des universités canadiennes. La SCGM serra fier d'annoncer les récipiendaires des distinctions honorifiques (prix, médailles et titres de "Fellow") lors du banquet de la conférence. Les prix pour les équipes gagnantes des concours étudiants seront également annoncés lors du même banquet.

C'est donc une période idéal pour s'impliquer et pour rester impliqués dans le SCGM. Nous devons travailler ensemble pour continuer de développer le génie au Canada et partout dans le monde.

Christine Q. Wu, CSME Président

Contributing to the CSME Bulletin

We welcome submissions of events, announcements, job postings, and feature articles relevant to mechanical engineering from researchers and engineers in Canada. Feature articles in forms of both review and research papers are welcome. The articles should be technical, general, and no more than 6000 words. If you are interested in submitting an article to the Bulletin, please contact the Editor at xiaodong.wang@ualberta.ca.

BECOME A CSME MEMBER

CONTACT:

JOHN PLANT, Executive Director CSME
1295 Highway 2 East,
Kingston,
Ontario, K7L 4V1

Phone: (613) 547-5989
Fax: (613) 547-0195
Email: csme@cogeco.com
or log on to: www.csme-scgm.ca

MEMBERSHIP FEES

Member $140
Fellow $175
Student $15

Kick-Off for Western University's CSME Chapter

By: Alicia Lenny, Logistics Co-ordinator, Western's CSME Student Chapter

The newly established Canadian Society for Mechanical Engineering (CSME) Student Chapter at Western University held its first event on Thursday, November 21 over the lunch hour. Approximately 120 students and several professors attended this seminar. Its purpose was to introduce students to CSME, connect them to the CSME community and teach them about design in industry, exposing them to opportunities post-graduation.

General information regarding CSME was presented while attendees enjoyed pizza for lunch. Students learned about the history and structure of CSME, and the benefits associated with being part of the society and Canadian community of mechanical engineers.

Our guest speaker, Gil Camirand, Manager (Product and Technology Development), of General Dynamics Land Systems (GDLS) in London, Ontario discussed the design process he uses to create armoured vehicles. Mr. Camirand spoke of the "v-method" which relates steps of the design process. The House of Quality was highlighted as a means of eliciting customer needs. In working with high profile customers, GDLS is careful to achieve customer's requirements while keeping costs low and functionality the primary objective.

After customer needs are established, vehicles are modeled using precise software. Mr. Camirand showed models of a recently developed vehicle, depicting how blasts affected parts of the vehicle. Using these models, vehicles are designed, or old vehicles redesigned. Mr. Camirand mentioned that, for GDLS "having validated models is invaluable", allowing proof of knowledge of superior designs.

We were also shown a set of "before and after" videos of completed tests with anthropomorphic test devices (ATD) inside. These videos showed how important testing was to the safety of vehicle occupants. In one case, the floor of the vehicle was destroyed, but after adjustments were made and more tests done, the floor provided extra support to the vehicle and the ATDs.

The industry application of design processes which are taught to students in Mechanical Engineering was relevant and interesting. Student feedback was positive, and many expressed interest in future events and further involvement in CSME. The Western Student Chapter of CSME will meet in January to plan for the 2014 Winter Term, and is looking forward to opportunities to expose students to industry standards and to connect them to their engineering community.

Special thanks to Brandon Tartaglia, President of the Student Chapter for his help and support in organizing the event.

Wind Energy Institute of Canada: Advancing the Development of Wind Energy Across Canada

By Carrie Houston, Project Engineer, Wind Energy Institute of Canada, North Cape, PE

The origin of the Wind Energy Institute of Canada (The Institute) is rooted in The Atlantic Wind Test Site (AWTS), an experimental wind turbine test site, founded in 1981 at the northernmost tip of Prince Edward Island (PEI). AWTS led Canada's research activities in wind energy through the 1980s and 1990s and began working with the Government of PEI in the late 1990s to develop the first megawatt-sized wind farm east of Quebec, installing a capacity of 10.56 MW by 2003 in PEI. With the success of this installation, the Government of PEI began to recognize the potential of wind energy as a reliable energy source and economic

energy across Canada through research, testing, training, and collaboration." As such, the Institute's areas of strategic focus include: research, development and demonstration; testing for certification; training, outreach and public education; and technical consultation and assistance.

The Wind Energy Institute of Canada's unique location at North Cape, PEI with 300 degrees of exposure to the Gulf of St Lawrence provides a harsh environment for wind turbine testing. This tough marine setting exposes turbine designs to high corrosion, sand, and salt rates, large winter/summer temperature

Figure 1. The Atlantic Wind Test Site (AWTS) depicted here in 1982, North Cape, Prince Edward Island.

development generator, and discussions on expanding AWTS's mandate began. Strategies initiated by the Government of PEI and the Atlantic Canada Opportunities Agency (ACOA) resulted in a Conceptual Plan for the Wind Energy Institute of Canada by 2005. In the fall of 2006, the Institute officially opened as a Not for Profit Organization governed by a volunteer Board of Directors.

The Wind Energy Institute of Canada now has a team of ten fulltime staff and operates under the following Mission Statement: "The Institute advances the development of wind

changes, and icing events producing valuable testing results over a wide range of conditions leading to greater confidence in certification of turbines entering the global market and varying environments.

The Institute is a highly collaborative organization with undertakes research, development and demonstration across a broad spectrum of activities such as, distributed generation, forecasting, wind-diesel systems, and wind-hydrogen applications. The Institute has an extensive history of small wind turbine

(turbines with a swept area of less than 200 square meters) testing and prototype development, and has more recently become active in the research, development and demonstration of large wind, with the commissioning of the Institute's 10 MW Wind Park in 2013. Additionally, by 2014, The Institute will have installed a 1 MW utility-sized battery storage system for testing in conjunction with the Wind Park.

Small Wind Turbine Testing

The Wind Energy Institute of Canada's small wind turbine testing program is in accordance with the International Electrotechnical Commission (IEC) 61400 standards, and can perform testing services to conform to the American Wind Energy Association (AWEA), British Wind Energy Association (BWEA), and the Class NK Japanese Standard. Specific tests performed can include: power performance, load measurement, power quality, acoustic noise emissions, duration, and safety. The Institute's testing services are mobile, however, small wind turbine test beds are available at the Institute's North Cape site. Small wind turbines currently under test at the North Cape site include: 2.5 kW, 25 kW, and 50 kW turbines. Other current small wind installations at the Institute include 5 kW and 10 kW wind turbines undergoing research and development on various aspects of their respective design features.

Figure 2. The Wind Energy Institute of Canada's North Cape wind turbine test site today.

Wind R&D Park and Storage System for Innovation in Grid Integration

The Institute's Wind R&D Park project was announced in 2010 when it was awarded a $12 million federal grant from the "Clean Energy Fund" to demonstrate the economic and technical feasibility of wind energy storage in Canada. This demonstration features five DeWind D9.2 wind turbines with a generating capacity of 10 MW, and incorporates a utility-sized 1 MW Battery Energy Storage System (BESS) from S&C Electric

Canada Ltd (S&C) and General Electric (GE). The 10 MW Wind Park was commissioned in April 2013 and has generated in excess of 11 GWh of power to date for the PEI electricity grid. Ground work is currently underway at the Wind Park substation for the battery storage installation. The project has also been supported by the Government of PEI with a $12.6M loan which will be repaid from the sale of power produced by the new infrastructure. With a focus on research, the project will add to Canada's understanding of the production, operation, storage and installation of small and large wind energy technologies.

Figure 3. The recently commissioned Wind R&D Park has a 10 MW capacity.

This new asset base will allow the Institute to expand its research mandate and provide sector enabling support helping manufacturers, governments, and academia evaluate and improve their technologies. The Wind R&D Park and Storage System will offer system operators and utilities a bench test environment for wind and storage systems that currently does not exist. The opportunities presented by this new installation will allow the Institute to expand its research role into:

- Optimization of wind forecasting and forecasting methodologies using real time data
- Voltage control
- Frequency regulation (primary regulation)
- Transmission network support to delay or avoid network upgrades
- Reserve capacity
- Grid integration issues
- Continued testing, research, development, and demonstration of wind technologies
- Storage facilities to mitigate energy intermittency, and
- Storage performance with respect to reliability and economics

Figure 4. Ground work underway for battery installation.

Figure 5. Battery Energy Storage System

The Battery Energy Storage System is composed of two primary components, namely, a Power Conversion System (PCS), supplied by S&C via its field-proven PureWave® Storage Management System (SMS), and battery modules supplied by GE. The batteries, consisting of sodium nickel chloride Durathon modules, represent the first such project for GE Energy Storage in Canada. The PureWave® SMS converts the energy generated by the wind turbines to direct current, which charges the batteries and when called upon, will reverse the flow to take the energy from the batteries and convert it into alternating current for use by the utility, Maritime Electric Company Limited, for sale to retail customers. As a demonstration project, the BESS will be operated in a number of ways to demonstrate the benefits of energy storage under varying scenarios. Operation in a time shift mode is a probable application, as demonstrated in Figure 6, where excess energy is stored in times of low demand and supplied for use in times of higher demand. Other demonstrations on power smoothing (Figure 7) and voltage control could also provide useful information for clients of such systems. Demonstration of these practical applications for energy storage systems will increase the acceptance and utilization of such systems and allow for integration of more renewable energy by utilities into the energy generation mix.

Figure 6. Time shifting opportunity example for PEI load. The battery storage system could be demonstrated to store energy when the wind power generation exceeds the demand load, and top up the wind energy production at the times when it does not meet the demand load.

Figure 7. Power smoothing of wind power generation through use of battery charging when the wind is high and discharging when the wind is low to reduce output fluctuations.

Academic Collaborations

Academic collaborations are a key component of the Wind Energy Institute's mandate of research, development and demonstration. The Institute acts as an enabler of industry-academic partnership in wind-related research. The Institute currently plays a role in the NSERC Wind Energy Strategic Network (WESNet), Canada's nation-wide wind energy research collective, a multi-partner alliance which includes leading researchers from 16 Canadian universities in six provinces, NRCan, Environment Canada, the Canadian Wind Energy Association, utility companies, and wind energy sector businesses. Under this initiative, The Institute has enabled researchers at the

Université de Laval to test their ice-free anemometer designs in the harsh conditions of The Institute's North Cape site.

The Institute is also collaborating with WESNet on the testing of a 10 kW wind turbine developed by the WESNet Team. The objective of the project is to develop, demonstrate, and evaluate an integrated small wind turbine package with advanced technologies to address the industry's need for high performance, low cost, small wind turbines. The turbine is currently installed at The Institute's North Cape site where performance data collection is underway to fine-tune the turbine's innovative technologies.

The Institute has recently signed a memorandum of understanding with the University of Western Ontario's WindEEE Research Institute with the intent to pursue cooperative relations in research and education of wind turbine technology. Collaboration from both organizations in providing services to small wind turbine manufactures in development of their product will lead to eventual testing leading to certification. Exchange of resources including personnel, expert knowledge and client referrals will build a diverse wind research and testing infrastructure.

Wind Energy Today and Into the Future

The Wind Energy Institute of Canada's work is contributing to a growing wind energy industry in Canada. According to the Canadian Wind Energy Association (CanWEA), there are currently 162 wind farms operating in Canada, with more than 3500 wind turbines installed, with a total generating capacity of 7,051 MW. This represents 3% of Canada's total electricity load, with an anticipated 1,500 MW capacity expected to be installed across the country within the next four years. The province of Prince Edward Island currently has 9 wind farms in operation, with 94 wind turbines with a generating capacity of 173.6 MW, representing over 30% of PEI's electricity load. A new 30 MW capacity wind farm is currently being installed in Hermanville, PE and is scheduled to be operational by the end of 2013.

The Wind Energy Institute of Canada has built a team of highly skilled and experienced technical staff, as well as, a collaborative network of academics and industry professionals dedicated to the development of the wind energy industry. The Institute actively seeks opportunities to work with partners in the development of technology, and provides fee for service technical consultation. For more information please visit www.WEICan.ca.
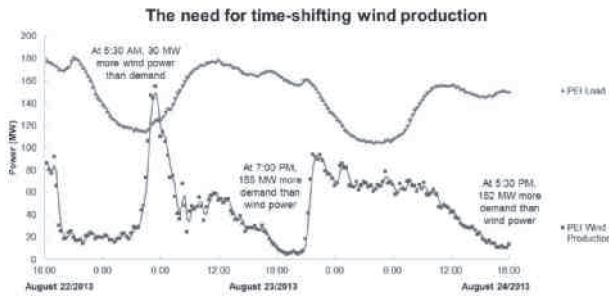
Figure 6. Time shifting opportunity example for PEI load. The battery storage system could be demonstrated to store energy when the wind power generation exceeds the demand load, and top up the wind energy production at the times when it does not meet the demand load.
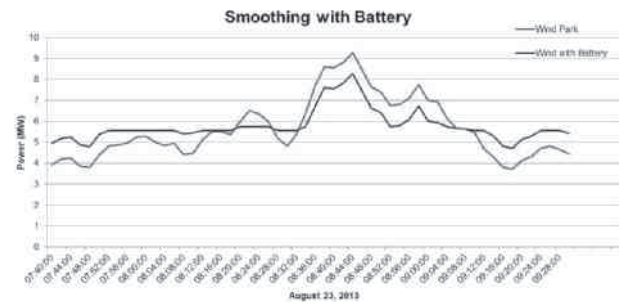

Figure 7. Power smoothing of wind power generation through use of battery charging when the wind is high and discharging when the wind is low to reduce output fluctuations.

Academic Collaborations

Academic collaborations are a key component of the Wind Energy Institute's mandate of research, development and demonstration. The Institute acts as an enabler of industry-academic partnership in wind-related research. The Institute currently plays a role in the NSERC Wind Energy Strategic Network (WESNet), Canada's nation-wide wind energy research collective, a multi-partner alliance which includes leading researchers from 16 Canadian universities in six provinces, NRCan, Environment Canada, the Canadian Wind Energy Association, utility companies, and wind energy sector businesses. Under this initiative, The Institute has enabled researchers at the Université de Laval to test their ice-free anemometer designs in the harsh conditions of The Institute's North Cape site.

The Institute is also collaborating with WESNet on the testing of a 10 kW wind turbine developed by the WESNet Team. The objective of the project is to develop, demonstrate, and evaluate an integrated small wind turbine package with advanced technologies to address the industry's need for high performance, low cost, small wind turbines. The turbine is currently installed at The Institute's North Cape site where performance data collection is underway to fine-tune the turbine's innovative technologies.

The Institute has recently signed a memorandum of understanding with the University of Western Ontario's WindEEE Research Institute with the intent to pursue cooperative relations in research and education of wind turbine technology. Collaboration from both organizations in providing services to small wind turbine manufactures in development of their product will lead to eventual testing leading to certification. Exchange of resources including personnel, expert knowledge and client referrals will build a diverse wind research and testing infrastructure.

Wind Energy Today and Into the Future

The Wind Energy Institute of Canada's work is contributing to a growing wind energy industry in Canada. According to the Canadian Wind Energy Association (CanWEA), there are currently 162 wind farms operating in Canada, with more than 3500 wind turbines installed, with a total generating capacity of 7,051 MW. This represents 3% of Canada's total electricity load, with an anticipated 1,500 MW capacity expected to be installed across the country within the next four years. The province of Prince Edward Island currently has 9 wind farms in operation, with 94 wind turbines with a generating capacity of 173.6 MW, representing over 30% of PEI's electricity load. A new 30 MW capacity wind farm is currently being installed in Hermanville, PE and is scheduled to be operational by the end of 2013.

The Wind Energy Institute of Canada has built a team of highly skilled and experienced technical staff, as well as, a collaborative network of academics and industry professionals dedicated to the development of the wind energy industry. The Institute actively seeks opportunities to work with partners in the development of technology, and provides fee for service technical consultation. For more information please visit www.WEICan.ca.

Sulphur Diffusion in β-NiAl and Effect of Pt additive: An ab inito Study

Kuiying Chen, Xijia Wu and Weijie Chen

National Research Council Canada, Aerospace Portfolio, Ottawa

ABSTRACT

Diffusivities of detrimental impurity Sulfur (S) in stoichiometric and Pt doped β-NiAl were evaluated using density functional theory calculations. The apparent activation energy and the pre-exponential factor of diffusivity via the next nearest neighbour (NNN) and interstitial jumps were evaluated to identify possible preferred diffusion mechanism(s). By calculating the electron localization function (ELF), the bonding characteristics of S with its surrounding atoms were assessed for the diffusion process. By comparison with the experimental results, the S diffusion through the NNN vacancy-mediated mechanism is found to be favoured. Addition of Pt in β-NiAl was found to significantly reduce the S diffusivity, and an associated electronic effect was explored. The elucidation of the above mechanisms may shed light on the development of new Pt-modified doped β-NiAl bond coats that can extend the life of oxidation resistant and thermal barrier coatings.

Key words: Sulfur, diffusivity, NiAl, Pt, ab initio calculations

1. INTRODUCTION

Thermal-barrier coatings (TBC), which consist of a thermal-insulating ceramic top (TC) coat and an oxidation-resistant metallic bond coat (BC), have long been served in advanced gas turbine engines to protect the hot-section components in hostile operating environments. These TBCs can be deposited by plasma spray processes and/or electron beam physical vapour deposition (EB-PVD) techniques, the latter being more often used for aero-engine applications, because the EB-PVD microstructure is more tolerant to thermomechanical fatigue [1].

The metallic bond coat (or BC) is an important constituent of the TBC system. It is often made of either platinum (Pt) modified nickel aluminide, β-(Ni, Pt)Al, or a multiphase MCrAlY (M = Ni and/or Co) alloy, which allows the formation of an alumina Al2O3 layer between the TC/BC interface to protect the BC and the substrate from further oxidation during the subsequent service exposure. Several failure mechanisms were proposed regarding the spallation of TBC off the substrate. The thermal stress concentration is the major cause arising from a mismatch in thermal expansion coefficients between the thermally grown oxide (TGO) Al2O3 and BC as TGO thickens.

It has been recognized that segregation of impurity sulphur (S) to the BC/TGO interface weakens the interface adhesion, as a result, leading to the interface embrittlement. It has also been reported that the S segregation can result in a void growth and coalescence at the interface, eventually leading to spallation of the TBC [2, 3, 4-17]. Desulfurizing was found to significantly improve the oxide adherence to the metal substrate [8, 17-24]. Although Pt does not form a sulphide, its addition to β-NiAl was shown to be capable of limiting the detrimental effects of S by increasing the oxide growth to fill up the voids and by reducing the S segregation rate to the interface [14, 17, 19, 25-27]. The role of Pt in β-(NiAl) phase-containing bond coat has been mostly thought to be lowering the chemical activity of Al, since Al forms a stronger bond with Pt than with Ni in β-NiAl [28]. The interesting question is how exactly Pt affects S diffusion. Limited experiments have shown that the effect of Pt on S diffusion is temperature-dependent [29, 30]. At elevated temperatures (T> ~1200 K), Pt was observed to reduce the S segregation rate.

To authors knowledge, the mechanisms of S diffusion in β-NiAl and with addition of Pt have not been fully understood at the microscopic scale. Since a full experimental characterization of S diffusion in β-NiAl with different additives is very difficult and costly, it is necessary to study possible microscopic scale mechanisms that govern S diffusion in doped/undoped β-NiAl. In this study, we carried out ab initio density functional theory calculations combined with the theory of atomic transportation in solid to investigate S diffusion in a clean and Pt dopedβ-NiAl. Particularly, the apparent activation energies and the diffusion coefficients are evaluated for S diffusion. Then, by comparing with experimental measurements, the favoured S-diffusion mechanism was identified. The results may shed some light on the understanding of the microscopic scale characteristics of S diffusion, and could provide guidance for future TBC development.

2. METHODS

Phenomenologically, diffusivity D is predicted by following the Arrhenius law:

$$D = D_0 \exp(-Q/k_B T) \qquad (1)$$

where D_0 is the pre-exponential factor, Q is the apparent activation energy for diffusion, k_B is the Boltzmann constant and T is the absolute temperature. The activation energy and the pre-exponential factor are often determined by fitting the experimentally measured diffusion rate vs. the inverse temperature relationship, regardless of the physical mechanisms.

In atomic transportation theory, the activation energy Q for diffusion is defined as the sum of migration energy E_{mig} (solute or impurity) of diffusing atom and the formation energy $E_{Vac}{}^f$ of point defect-solute/impurity complex. The formation energy of a defect/additive (A)-containing system such as β-NiAl is defined as:

$$E_F = \Delta E^F_{Ni_{x'}Al_{y'}A_m} - \frac{N_d}{N}\Delta E^F_{Ni_X Al_Y} \qquad (2)$$

where $N = x+y$ is the total number of constituent atoms in the stoichiometric β-NiAl, and $N_d = x'+y'+m$ is the total number of atoms for a defect/additive-containing system. In both cases, x, y, x', y' stand for Ni and Al atoms in stoichiometric and defect/additive containing structure, respectively, while m is the number of defects/additives. ΔE^F is the formation energy of the alloy evaluated as:

$$\Delta E_{Ni_X Al_Y} = E_{Ni_X Al_Y} - xE(Ni) - yE(Al) \qquad (3)$$

for stoichiometric β-NiAl that possesses x Ni and y Al atoms, in which E_{NixAly} represents its total energy in the supercell. $E(Ni)$ and $E(Al)$ are the energies of single Ni and Al atoms, respectively. Similarly, for β-NiAl that contains x'(Ni), y'(Al) and m additives/vacancies A, the formation energy of the alloy becomes [32, 33]:

$$\Delta E_{Ni_{x'}Al_{y'}A_m} = E_{Ni_{x'}Al_{y'}A_m} - x'E(Ni) - y'E(Al) - mE(A) \qquad (4)$$

where $E(A)$ is the energy of the defect/additive (A) [34] ($E(A)$=0 eV, if A is a vacancy). The formulas (2)-(4) have been previously validated for diffusion calculations [32,33], and will be used in the present calculations for S diffusivities in β-NiAl.

Based on Einstein's random walk model, within the classical limit, the pre-exponential factor D_0 in the diffusion coefficient D is defined as:

$$D_0 = \frac{1}{6}fn\nu a^2 \exp(\frac{\Delta S^{vib}_m}{k_B}) \qquad (5)$$

where n is the number of equivalent jump paths depending on the crystalline structure, a is the jump distance, ν is the effective atom jump frequency, is the change in vibrational

entropy of migration, and f is the correlation factor. The correlation factor can be defined as the probability of a successful jump, which is equal to 1 ($f = 1$) for uncorrelated jumps and a value smaller than one, $f < 1$, for correlated jumps. The effective jump frequency ν and the vibrational entropy are calculated by evoking the harmonic transition state theory. At the high temperature limit, i.e., $hw/k_B T \ll 1$, only phonon contributions are considered. The vibrational entropy of a series of harmonic oscillators containing N atoms is calculated as:

$$S^{vib}_m = -k_B \sum_i^{3N-3} \ln\left(\frac{hw_i}{k_B T}\right) + 3Nk_B \qquad (6)$$

where w_i is the normal vibrational frequency, h is the Plank constant. To calculate the effective atomic jump frequency ν, the Vineyard expression in terms of vibrational frequencies at the initial and transition states of the migrating atom is used [35]:

$$\nu = \frac{\sum_i^{3N_d-3} w_i^{init}}{\sum_i^{3N_d-4} w_i^{trans}} \qquad (7)$$

The denominator of the jump frequency contains one less vibrational frequency at the saddle point since one vibrational degree of freedom is converted into a translational degree of freedom due to the motion along the reaction path [36]. Finally substituting Eqs (5), (7) into Eq. (1), the diffusion coefficient of S can be evaluated as:

$$D = \left(\frac{n}{6}fa^2 \frac{\sum_i^{3N_d-3} w_i^{init}}{\sum_i^{3N_d-4} w_i^{trans}} \exp(\frac{\Delta S^{vib}_m}{k_B})\right) \exp(-\frac{E_M + E_F}{k_B T}) \qquad (8)$$

Eqs. (2)-(8) allow the analytical evaluation of diffusivity without experimental measurements as inputs.

2.2. Ab initio Methods

In the present study at the microscopic scale, two super-cell models, one with 55 lattice sites, composed of 27 Ni, 27 Al, and 1S, and the other with 129 lattice sites, composed of 64 Ni, 64 Al and 1 S, are constructed to isolate possible interactions of the impurity with its periodic images. To fully simulate the atomic diffusion jumps, spin-polarized density functional theory calculations (DFT) are performed using the Vienna *Ab initio* simulation package (VASP) within a plane-wave basis sets [37]. The Perdew-Wang generalized gradient approximation (GGA) is used to calculate the electron exchange and correlation energy [38]. The projector augmented wave (PAW) potentials are used to describe the interactions of valence electrons with the ion and core electrons for all elements [39], where Ni $4s^2 3d^8$, Al $3s^2 3p^1$, Pt $6s^2 5d^2$ and S $3s^2 3p^4$, electrons are treated as valence.

For an interstitial diffusion of S, the 55-atom supercell was tested and found to be large enough to isolate the diffusing elements in the periodic images. For vacancy-mediated diffusion of S, the 53-atom supercell containing

a single vacancy with the S atom occupying the vacancy site was found to be capable of isolating the diffusing atom interactions between periodic images. The Brillouin zone integration is performed using a centered gamma point 6 × 6 × 6 Monkhorst Pack grid that yields 54 irreducible k-points [40]. The occupation of electronic states is determined according to the first order Methfessel-Paxton scheme with a smearing width of 0.2eV. A kinetic energy cutoff of 350 eV is used for all total energy calculations.

In all calculations, the equilibrium lattice constant for the stoichiometric β-NiAl was obtained by fully relaxing the volume of the supercell model. Starting with the experimental lattice constant a_0 = 2.887 Å, the equilibrium is defined as the forces on the ions becoming less than the threshold value of 0.01eV/Å for formation energy calculations, and 0.03eV/Å for diffusion calculations. It was previously shown that the reduced threshold has a negligible impact on the calculated migration energy [41]. The lattice parameter is calculated as 2.891 Å, in excellent agreement with the experimental value, and is used for all subsequent diffusion calculations.

The migration energy of S diffusion, defined as the difference between the energy at the saddle point and at the initial stable state, is calculated using the climbing nudged elastic band method (CINEB) [42-45]. In this method, for a given diffusion path with known initial and final minimum energies, a series of images are generated by a linear interpolation between the two end states. The images, which are connected through imaginary springs, are allowed to relax until the Hellmann-Feynman forces on atoms are less than the threshold values. By inverting the forces on the highest energy image, these images are made to climb along the minimum energy path (MEP) to reach the saddle point. To calculate the phonon frequencies w_i and w_i at the initial and saddle points respectively, the *fitfc* utility that uses the direct force constant supercell approach in the Alloy Theoretic Automated Toolkit (ATAT) package [46] is implemented with a displacement of ±0.05Å at the Γ point. [47]. Within the supercell method, from the fully relaxed structure, the positions of the atoms are perturbed and the new energies and inter-atomic forces are calculated without relaxing any degrees of freedom.

To study possible electronic related mechanisms that may govern the diffusion process, the electron localization function (ELF) is evaluated for S diffusion in β-NiAl and Pt doped β-NiAl as well. The ELF amplifies the bonding features, and allows one to analyze the electron distribution on an absolute scale, ELF is defined as:

$$ELF = \frac{1}{1+\left(\dfrac{D(\vec{r})}{D_h(\vec{r})}\right)^2} \qquad (9)$$

With

$$D(\vec{r}) = \frac{1}{2}\nabla_{\vec{r}}\nabla_{r^1}\rho(\vec{r},r^1)|_{\vec{r}=r^1} - \frac{1}{8}\frac{|\nabla n(\vec{r})|^2}{n(\vec{r})} \qquad (10)$$

and

$$D_h(\vec{r}) = \frac{3}{10}(3\pi^2)^{2/3}n(\vec{r})^{5/3} \qquad (11)$$

where ρ is the first-order reduced (spin-integrated) density matrix; $D(\vec{r})$ is the von Weizsäcker kinetic energy functional which corresponds to the ground state kinetic energy density of a non-interacting bosonic system at density $n(\vec{r})$, and $D_h(\vec{r})$ is the kinetic energy density of a uniform electron gas with a spin-density equal to the local value of $n(\vec{r})$. The ELF value is 0.5 for a homogenous electron gas and can increase to ~1.0 for electrons paired in a covalent bond or a highly localized, unpaired electron dangling bond. The ELF values below 0.5 are less readily understandable. These can correspond to regions of very low electron density. For more details on ELF and its derivation, see reference [48].

3. RESULTS AND DISCUSSIONS

β-NiAl possesses an ordered B2-CsCl, body centered cubic (BCC) structure, which consists of two interpenetrating Ni and Al simple cubic sub-lattices. As shown in Fig. 1, at the stoichiometric composition, the Al atoms occupy the corner sites (β-sites) and the Ni atoms occupy the body-centered sites (α-sites) in the unit cell. There are two distinct interstitial sites, at which an interstitial impurity S atom can occupy, the tetrahedral (Figure 1(b)-blue) and the octahedral (Figure 1(b)-red). For sulphur atom, due to its smaller radius and higher diffusion rate as compared to Ni and Al atoms, it was proposed that it would prefer to occupy interstitial sites [29]. Finally, the preferred substitutional site for Pt atom in β-NiAl alloy is determined to be the Ni site [49] by *ab initio* DFT calculations.

At elevated temperatures, deviations from the ideal β-NiAl structure may be observed due to the formation of point defects in the alloy. Vacancies and antisite atoms constitute these point defects. A vacancy is the absence of an atom from its sublattice denoted as V_{Ni} and V_{Al} for Ni and Al vacancies, respectively. An antisite atom is said to be formed when a Ni(Al) atom resides on an Al(Ni)-site symbolized by $Ni_{Al}(Al_{Ni})$. In order to determine the most favourable substitutional site of S, the formation energy of NiAl with a S atom substituting a Ni or an Al atom is calculated separately. As given in Table 1, a S atom at an Al site is found favourable. Thus the vacancy-mediated diffusion by a symmetric next nearest neighbour (NNN) jump from one Al sublattice site to another is considered as a potential S diffusion path.

The formation energy of NiAl with one S atom occupying a tetrahedral/octahedral interstice is evaluated. The results show that the structure with a S at the tetrahedral-site has a lower energy, as seen in Table 1. Therefore, the tetrahedral site is considered as the occupation site for the impurity S,

and atoms located on the S diffusion plane are referred to as $X^{A,M,N,Q}$ according to Figure 1(c). In the subsequent sections, we will discuss sulphur diffusion via both vacancy-mediated NNN and interstitial paths, evaluate diffusivities and identify the most favourable diffusion mechanism in -NiAl.

3.1. Vacancy-mediated S diffusion

3.1.1 Next nearest neighbour (NNN) diffusion of S in b-NiAl

As shown in Figure 2, the nudged elastic band (NEB) calculations for S diffusion by a NNN jump in NiAl (Figure 1d) results in a migration energy barrier of 0.4765 eV. The calculated activation energy of 3.5665 eV compares well with the experimental value of 2.26eV, reported by Rivoaland *et. al.* [29]. Combining the calculated pre-exponential factor D_0 of 0.014 with the activation energy in Eq. (1), yields the following prediction for the NNN S diffusion:

$$D_S^{NNN} = 0.014\exp(-\frac{3.5665}{k_BT})(cm^2/s) \qquad (12)$$

The diffusion coefficient given in Eq. (12) is plotted in Figure 3. At 1273 ^{0}C, the calculated diffusion coefficient D = 2×10^{-9} cm²/s agrees well with a recent experimental data of $D = 1\times10^{-9}$ cm²/s [31].

To probe possible electronic level effects associated with the diffusion process, the ELF is calculated for the NNN diffusion path. At the initial configuration, the S atom is displaced towards four neighbouring Ni atoms (on two adjacent planes but only two are shown in Figure 4 for one plane). During the transition state, S becomes equidistant with all four Ni atoms as determined from the electron localization between S-Ni atoms. In agreement with the ELF plot, the calculated atomic separations also indicate the displacement of S towards the vacancy, reducing four Ni-S separations to 2.27Å and increasing the other four to 2.81Å from the unrelaxed Ni-S separations of 2.5Å. During the transition, the shortest four Ni-S bonds lengths are reduced to 2.17Å, while the other four break off. At any stage during S diffusion, no bond formation is observed between S and Al atoms.

3.1.2 Effect of Pt on S NNN diffusion

In order to examine possible effects of Pt on the NNN S diffusion, one Ni atom (denoted by Ni^A) which is the nearest neighbour to both S_{Al} and V_{Al} is replaced by a Pt atom. The presence of Pt is found to increases the activation energy by 0.3785 eV, and slightly decreases the pre-exponential factor, Table 1, leading to a diffusion coefficient:

$$D_S^{NNN(Pt)} = 0.0095\exp(-\frac{3.94505}{k_BT})(cm^2/s) \qquad (13)$$

The higher activation energy combined with the smaller pre-exponential factor results in a decreased S diffusion rate as compared to that of the pure β-NiAl as shown in the Arrhenius type plot, Figure 3.

At the initial state, due to the presence of Pt in between the S and vacancy, one can see that S does not relax towards the vacancy. Instead, it displaces away from Pt, Figure 4. Such behaviour and the electron delocalization suggest that an initial repulsion exists between these atoms. At the saddle point, S diffuses through the Ni-plane that contains the Pt atom. S displaces away from Pt towards the opposite Ni, disrupting the order at this layer. Although there is a general repulsive behaviour between Pt and S, the increased electron localization at the transition state between these atoms can be an indicative of a weak S-Pt interaction.

It was also observed that S displaces away from Pt during the relaxation, elongating their separation from 2.27Å to 2.77Å as compared to the Ni^A-S bond. Due to this asymmetric configuration, one of the Ni-S bonds in NNN Ni does not form in the Pt-doped structure, and two additional Al-S bonds with lengths 2.71Å are observed. At the saddle point, the two additional Al-S and three Ni-S bonds are broken, and the Pt-S bond length remains larger compared to its counterpart, Ni^A-S bond in NiAl. Therefore, it can be concluded that the increased migration barrier is due to the repulsive Pt-S interaction since S is diffusing through a Pt-containing plane.

In general, at lower temperatures, a low point defect concentration may exist in β-NiAl. At elevated temperatures, however, formation of vacancies and antisite defects become more prominent. Thus it can be expected that at elevated temperatures, with abundant vacancies, the vacancy-mediated S diffusion via a NNN jump is naturally preferred. This phenomenon can be rationalized by examining the Arrhenius plots, Figure 3. Furthermore, it can be seen that at elevated temperatures, the DFT calculations show that Pt reduces the D diffusion rate in the NNN mechanism.

Recent experiments conducted by Christien et al. [30] showed that the diffusivities of S in both NiAl and NiPtAl crossed over each other at around ~1200 K, as shown in Figure 3, the mechanism causing this transition was, however, left unexplained. As discussed, at low temperatures, due to the low concentration of point defects, such as vacancies, the short-circuit diffusions via grain boundaries, dislocation pipelines and voids play major roles. At elevated temperatures, due to the high concentration of vacancies, the diffusion via the NNN mechanism can be consequently favored. Experimental data in figure 3 illustrates that at elevated temperatures, Pt reduces the S diffusivity in agreement with the DFT calculations. The implication of this result indicates that Pt shows the capability of slowing the impurity S diffusion, thus is capable of preventing S diffusing towards the TGO/BC interface from substrate, thereby diminishing its detrimental effect on TGO/BC interface adhesion. This necessarily exhibits the positive effect of Pt in the TBC

system. In real materials, however, S diffusion rates depend on the concentrations of the participating elements, which are not faithfully reflected in the simplified atomistic model constructed for the present study. Christien et al. [30] conducted the experiments on polycrystalline NiAl and NiPtAl coatings that also contained Ta, W and La, etc. The measured diffusivities essentially represent a mixture of data via different mechanisms including the NNN, grain boundaries and dislocation pipeline. Therefore, the present model is by no means matching the complexity of the real materials, which was already reflected by lower diffusivity values through DFT calculations than the experimentally observed in figure 3. Nonetheless, the present diffusion models account for the potential contributing mechanisms.

3.2 Interstitial S diffusion

In order to explore the possible interstitial diffusion of S in β-NiAl, as an example, two sublattice planes in β-NiAl: 1) the Ni-sublattice plane (NSP) on which all atoms on the diffusion plane are Ni atoms, and 2) the Al-sublattice plane (ASP) are constructed. These two planes correspond to different nearest neighbour configurations for S diffusion. Since the migration energy is governed by interactions of S with its immediate surroundings on the diffusion plane, S diffusion by NSP and ASP jumps will be discussed separately.

3.2.1 NSP and ASP jumps

Interstitial S diffusion on an NSP involves diffusion of the S atom from one tetragonal site, above a Ni-Ni bridge, onto another tetragonal site as demonstrated in Figure 1 (c). For stoichiometric β-NiAl, the MEP is symmetric with a migration barrier of 0.036 eV and the vibrational entropy and frequency result in a pre-exponential factor D_0=1.5×10^{-5} cm^2/s.

In the ASP diffusion mechanism, S hops from one tetrahedral site, above an Al-Al bridge, to another via the interstitial diffusion. The NEB calculations for ASP jump result in a migration barrier of 0.014 eV, which is much smaller than that for NSP, and the frequency calculations yield a pre-exponential factor, D_0 = 2.3×10^{-5} cm^2/s. These two parameters together determine the diffusivity at a given temperature, according to Eq. (1).

Table 1 shows the calculated apparent activation energy of S diffusion via an interstitial mechanism for both scenarios. The calculated activation energies are considerably larger than through the NNN mechanism, and together with the calculated diffusivities it indicates that the interstitial diffusion mechanism of S is not favored in -NiAl. As discussed in the previous sections, at low temperatures where the concentration of point defects is low, the short-circuit diffusion may dominate the S diffusion in -NiAl. Therefore, it is necessary to investigate the S diffusion via grain boundary mechanism, and examine how exactly Pt affects the S diffusion. This on going work along with the obtained results will identify the most favourable diffusion

mechanism of S in -NiAl. These results are expected to shed light on the development of oxidation-resistant coatings and TBC.

4. CONCLUSIONS

Ab initio DFT calculations were performed to study S diffusion in β-NiAl and to examine the effect of Pt on its diffusivities. A number of possible diffusion mechanisms, i.e., the NNN, the interstitial via both NSP and ASP, were evaluated. By comparing with the experimental apparent activation energies and diffusivities, it is suggested that S diffusion in -NiAl predominantly occurs by the vacancy-mediated NNN mechanism, and addition of Pt reduces its diffusivity. The ELF plots together with atomic separations indicate that S does not prefer to be in the close proximity of Pt. This atomic-level mechanism points out that Pt prevents S from segregating to the BC/TGO interface, resulting in reduction of S concentration at the metal/oxide interface, thus diminishing the S detrimental effect on the interface adhesion.

References

[1] M.J. Stiger, N.M. Yanar, M.G. Topping, F.S. Pettit, and G.H. Meier, Thermal Barrier Coatings for the 21st Century, *Z. Metallkd.*, **90** (1999) 1069-1078.

[2] S.M. Meier, D.M. Nissley, K.D. Sheffler, and T.A. Cruse, Thermal Barrier Coating Life Prediction Model Development, Paper #91-GT-40, International Gas Turbine and Aeroengine Congress and Exposition, Orlando, FL, June 3-6, 1991. (Trans. ASME, 1992, vol. 114, pp. 258-63)

[3] M. Gell, K. Vaidyanathan, B. Barber, J. Cheng, and E. Jordan, Mechanism of Spallation in Platinum Aluminide/Electron Beam Physical Vapor–Deposited Thermal Barrier Coatings, *Metallurgical and Materials Transactions*, **30A** (1999) 427-435.

[4] P.K. Wright and A.G. Evans, Mechanisms governing the performance of thermal barrier coatings, *Current Opinion in Solid State and Materials Science*, 4 (1999) 255–265.

[5] W. Lee, I. Wright, B. Pint, Y. Zhang, and P. Liaw, "Effects of sulfur impurity on the scale adhesion behavior of a desulfurized Ni-based superalloy aluminized by chemical vapor deposition," *Metallurgical and Materials Transactions* A, **vol. 29**, pp. 833–841, 1998.

[6] J. A. Haynes, "Potential influences of bond coat impurities and void growth on premature failure of EB-PVD TBCs," *Scripta Materialia*, vol. 44, no. 7, pp. 1147 – 1152, 2001.

[7] I. Rivoaland, V. Maurice, P. Josso, M.-P. Bacos, and Marcus.P., "The effect of sulfur segregation on the adherence of the thermally-grown oxide on NiAl - II: The oxidation behavior at 900 C of standard, desulfurized of sulfur-doped NiAl(001) single-crystals," *Oxidation of Metals*, vol. 60, no. 1/2, p. 159, 2003.

[8] A.W. Funkenbusch, J.G. Smeggil, and N.S. Bornstein, Reactive Element-Sulfur Interaction and Oxide Scale Adherence, *Metallurgical Transactions*, 16A (1985) 1164-1166.

[9] J.G. Smeggil, Some comments on the role of yttrium in protective oxide scale adherence, *Materials Science and Engineering*, **87** (1987) 261-265.

[10] J.L. Smialek, Adherent Al2O3 scales formed on undoped NiCrAl alloys, *Metallurgical Transactions*, **18A** (1987) 164-167.

[11] A.S. Khanna, H. Jonas, W.J. Quadakkers, Use of acoustic emission technique to

study the spalling behaviour of oxide scales on Ni-10Cr-8Al containing sulphur and/or yttrium impurity, *Werkstoffe und Korrosion*, **40** (1989) 552-558.

[12] J.L. Smialek, Effect of Sulfur Removal on Al2O3 Scale Adhesion, *Metallurgical Transactions*, **22**A (1991) 739-752.

[13] H.J. Grabke, D. Wiemer, H. Viefhaus, Segregation of sulfur during growth of oxide scales, *Applied Surface Science*, **47** (1991) 243-250.

[14] J.L. Smialek, D.T. Jayne, J.C. Schaeffer, W.H. Murphy, Effects of hydrogen annealing, sulfur segregation and diffusion on the cyclic oxidation resistance of superalloys: a review, 253 (1994) 285-292.

[15] J.L. Smialek and B.K. Tubbs, Effect of Sulfur Removal on Scale Adhesion to PWA 1480, *Metallurgical and Materials Transactions*, **26A** (1995) 427-435.

[16] W.Y. Lee, Y. Zhang, I.G. Wright, B.A. Pint, and P.K. Liaw, Effect of sulfur impurity on the scale adhesion behavior of a desulfurized Ni-based superalloy aluminized by chemical vapor deposition, *Metallurgical and Materials Transactions*, **29A** (1998) 833-841.

[17] J.A. Haynes, B.A. Pint, K.L. More, Y. Zhang, and I.G. Wright, Influence of Sulfur, Platinum, and Hafnium on the Oxidation Behavior of CVD NiAl Bond Coatings, *Oxidation of Metals*, **58** (2002) 513-544.

[18] Y. Cadoret, M.-P. Bacos, P. Josso, V. Maurice, P. Marcus, and S. Zanna, Effect of Pt Additions on the Sulfur Segregation, Void Formation and Oxide Scale Growth of Cast Nickel Aluminides, *Materials Science Forum*, 461-464 (2004) 247-254.

[19] P.Y. Hou and K.F. McCarty, Surface and interface segregation in -NiAl with and without Pt addition, *Scripta Materialia*, **54** (2006) 937–941.

[20] P.Y. Hou, T. Izumi, B. Gleeson, Sulfur Segregation at Al2O3/ -Ni + '-Ni3Al Interfaces: Effects of Pt, Cr and Hf Additions, *Oxidation of Metals*, **72** (2009) 109-124.

[21] T. Gheno, D. Monceau, D. Oquab, and Y. Cadoret, "Characterization of sulfur distribution in Ni-Based superalloy and thermal barrier coatings after high temperature oxidation:A SIMS analysis," *Oxidation of Metals*, vol. **73**, p. 95, 2010.

[22] J. Smialek, "Nonprotective Alumina Growth in Sulfur-Doped NiAl(Zr)," NASA/TM, vol. 209800, 2000.

[23] E. Schumann, J. Yang, and M. Graham, "Direct Observation of the interaction of yttrium and sulfur in oxidized NiAl," *Scripta Materialia*, vol. 34, no. 9, p. 1365, 1996.

[24] E. Schumann, J. Yang, M. Graham, and M. Ruhle, "The effect of Y and Zr on the oxidation of NiAl," *Materials and Corrosion*, vol. **47**, p. 631, 1996.

[25] Y. Zhang, W. Lee, J. Haynes, I. Wright, K. Cooley, and P. Liaw, "Synthesis and cyclic oxidation behavior of a (Ni, Pt) Al coating on a desulfurized Ni-base superalloy," *Metallurgical and Materials Transactions* A, vol. 30, pp. 2679–2687, 1999.

[26] F. Qin, C. Jiang, J.W. Anderegg, C.J. Jenks, B. Gleeson, D.J. Sordelet, P.A. Thiel, Segregation of Pt at clean surfaces of (Pt, Ni)3Al, *Surface Science*, **601** (2007) 376-380.

[27] Y. Cadoret, D. Monceau, P. Bacos, P. Josso, and V. e. a. Maurice, "Effect of platinum on the growth of the oxide scale formed on cast nickel aluminide intermetallic alloys," Oxidation of Metals, vol. 64, no. 3-4, p. 185, 2005.

[28] B. Gleeson, W. Wang, S. Hayashi, D. Sordelet, Effects of platinum on the interdiffusion and oxidation behavior of Ni-Al-based alloys, Materials Science Forum, 461-464 (2004) 213-222.

[29] I. Rivoaland, V. Maurice, P. Josso, M.-P. Bacos, and Marcus.P., "The effect of sulfur segregation on the adherence of the thermally-grown oxide on NiAl - I:Sulfur segregation on the metallic surface of NiAl(001) Single crystals and at NiAl(001)/Al 2 O 3 interfaces," Oxidation of Metals, vol. 60, no. 1/2, p. 137, 2003.

[30] Christien,F. and Pouteau,P. and Le Gall,R. and Saindrenan,G. and Jaslier,Y., "Segregation du soufre a la surface d'un materiau multicouche. Role du platine dans l'ecaillage des couches d'oxyde protectrices," *J. Phys. IV France*, vol. 10, p. 173, 2000.

[31] P. Hou and K. Primak, "Interfacial segregation, pore formation and scale adhesion on NiAl alloys," *Oxidation of Metals*, vol. 63, no. 1-2, p. 113, 2005.

[32] X.-L. Hu, Y. Zhang, G.-H. Lu, T. Wang, P.-H. Xiao, P.-G. Yin, and H. Xu, "Effect of O impurity on structure and mechanical properties of NiAl intermetallics: A first-principles study," *Intermetallics*, vol. 17, no. 5, pp. 358 – 364, 2009.

[33] P. Korzhavyi, I. Abrikosov, and B. Johansson, "Ab initio study of vacancies in metals and compounds," in Properties of complex inorganic solids 2 (A. Meiker, A. Gonis, A. Turchi, and K. Rajan, eds.), p. 63, Kluwer Academic/Plenum Publishers, 2000.

[34] Q. Xu and A. Van der Ven, "First-principles investigation of migration barriers and point defect complexes in B2-NiAl," *Intermetallics*, vol. 17, p. 319, 2009.

[35] G. Vineyard, "Frequency factors and isotope effects in solid state rate processes," *J. Phys. Chem. Solids*, vol. 3, no. 1-2, pp. 121–127, 1957.

[36] Y. Mishin, A. Lozovi, and A. Alavi, "Evaluation of diffusion mechanisms in NiAl by embedded-atom and first-principles calculations," *Phys. Rev.* B, vol. 67, no. 014201, 2003.

[37] G. Kresse and J. Furthmuller, "Efficient Iterative Schemes for ab initio Total-energy Calculations Using a Plane-wave Basis Set," *Phys. Rev.* B, vol. 54, no. 16, p. 11169, 1996.

[38] J. Perdew, K. Burke, and Y. Wang, "Generalized gradient approximation for the exchange-correlation hole of a many-electron system," *Phys. Rev.* B, vol. 54, no. 23, p. 16533, 1996.

[39] J. D. Kresse, G., "From ultrasoft pseudopotentials to the projector augmented-wave method," *Phys. Rev.* B, vol. 59, no. 3, pp. 1758–1775, 1999.

[40] H. Monkhorst and J. Pack, "Special points for Brillouin-zone integrations," Phys. Rev. B, vol. 13, no. 12, p. 5188, 1976.

[41] K. Marino and E. Cater, "The effect of platinum on Al diffusion kinetics in -NiAl: Implications for thermal barrier coating lifetime," *Acta Mater*, vol. 58, p. 2726, 2010.

[42] H. Jonsson, G. Mills, and K. Jacobsen, "Nudged Elastic Band Method for Finding Minimum Energy Paths of Transitions," in Classical and Quantum Dynamics in Condensed Phase Simulations (B. Berne, G. Ciccotti, and D. F. Coker, eds.), p. 385, World Scientific, 1998.

[43] G. Henkelman, B. Uberuaga, and H. Jonsson, "A climbing image nudged elastic band method for finding saddle points and minimum energy paths," *J. Chem. Phys.*, vol. 113, no. 22, p. 9901, 2000.

[44] G. Henkelman and H. Jonsson, "Improved tangent estimate in the nudged elastic band method for finding minimum energy paths and saddle points," *J. Chem. Phys.*, vol. 113, no. 22, p. 9978, 2000.

[45] G. Henkelman, G. Johannesson, and H. Jonsson, "Methods for Finding Saddle Points and Minimum Energy Paths," in Theoretical Methods in Condensed Phase Chemistry (S. Schwartz, ed.), vol. 5, Springer, 2001.

[46] A. Van de Walle, M. Asta, and G. Ceder, "The Alloy Theoretic Automated Toolkit: A User Guide," *CALPHAD* journal, vol. 26, p. 539, 2002.

[47] S. Wei and M. Chou, "Ab initio Calculation of Force Constants and Full Phonon Dispersions," *Phys. Rev. Lett*, vol. 69, no. 19, p. 2799, 1992.

[48] A. Becke and E. K.E., "A simple measure of electron localization in atomic and molecular systems," *J. Chem. Phys*, vol. 92, p. 5397, 1990.

[49] C. Jiang, "Site preference of transition-metal elements in B2 NiAl: A comprehensive study," *Acta Mater.*, vol. 55, p. 4799, 2007.

[50] K. Marino and E. Cater, "The effect of platinum on defect formation energies in β-NiAl,"*Acta Mater*, vol. 56, no. 14, p. 3502, 2008.
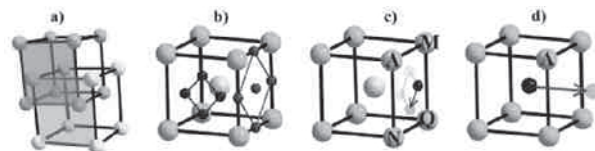

Figure 1: Stoichiometric NiAl; Al atoms occupy the corner sites (β-sites)(green) and Ni atoms occupy the body-centered sites (α-sites)(yellow), a) The Ni sublattice plane (NSP) in orange and the Al sublattice plane (ASP) in green. b) tetragonal interstitial sites in blue and octahedral interstitial sites in red. c) Atom A represents the atom that is being substituted. d) NNN diffusion.

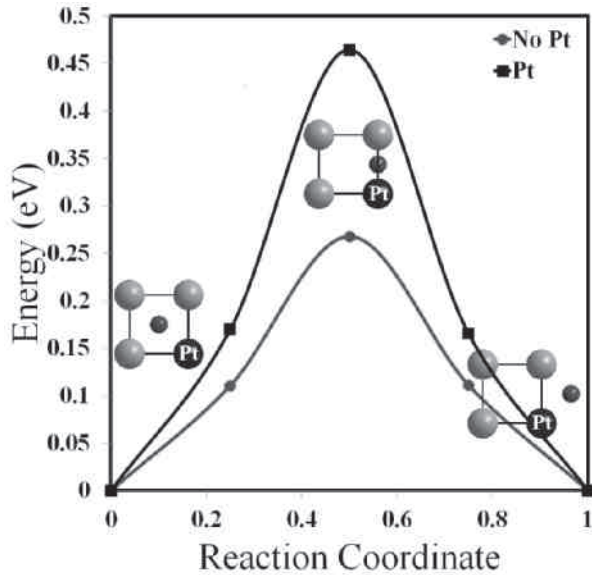Figure 4: The initial and transition state of ELF plots for S NNN diffusion in NiAl and in Ni(Pt)Al.

Figure 2. *Migration energy E_{mig} calculated by nudged elastic band for NNN S diffusion and the effect of Pt on E_{mig}.*

Table 1: The migration energy E_{mig}, formation energy E_f, activation energy Q and

pre-exponential factor D_0 for of S diffusion.

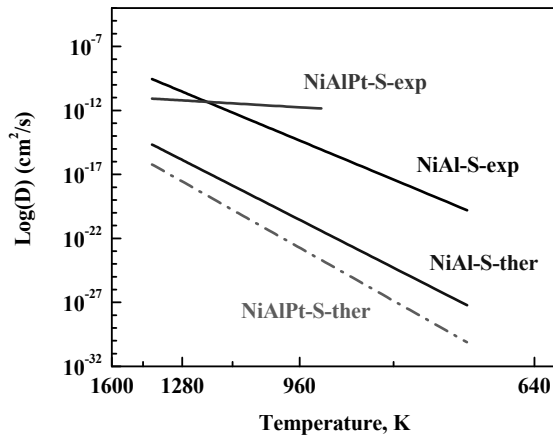|	E_{mig} (eV)	E_f (eV)	Q (eV)	D_0 (cm²/s)
NiAl (NNN)	0.4765	3.09	3.5665	1.4×10^{-2}
NiAlPt (NNN)	0.67505	3.27	3.94505	9.5×10^{-3}
NiAl [30]			2.91	8.4
NiAlPt [30]			0.41	2.5×10^{-10}
NiAl (NSP)	0.036	4.973	5.009	1.5×10^{-5}
NiAlPt (ASP)	0.014	5.13	5.144	2.3×10^{-5}

Figure 3 *Diffusion coefficient of S in β-NiAl. The black solid curve (NiAl-S-exp) represents experimental measurement without Pt addition [30]; the red solid curve (NiAlPt-S-exp) stands for the experiment value with Pt addition [30]. The blue solid line (NiAl-S-ther) is referred to the calculated S diffusivity without Pt addition, while the dash green line (NiAlPt-S-ther) plots the calculated S diffusivity considering Pt effect. Both calculated results are under the NNN mechanism.*
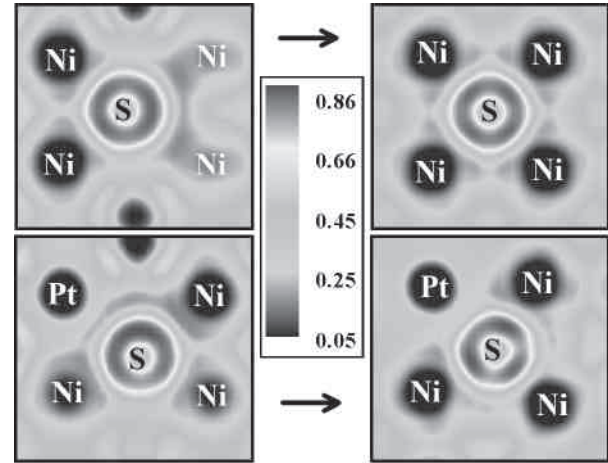
CSME International Congress 2014

The CSME Congress 2014 will be held from June 1 to June 4 at the University of Toronto St. George campus in Toronto. The Department of Mechanical & Industrial Engineering, Faculty of Applied Science & Engineering will host the congress.

The CSME International Congress is the flagship conference of the CSME and is held biannually. CSME International Congress promotes the communication and transfer of technology among industry, government agencies, universities and R&D laboratories. The CSME Congress offers a platform for national and international Mechanical Engineering experts to meet, exchange information, discuss recent research challenges, and explore problems of practical importance to the profession and its related fields.

The CSME CONGRESS encompasses all aspects of Mechanical Engineering, including the following:

- Aerospace and Aeronautics
- Biomechanics and Bioengineering
- Controls, Mechatronics, Robotics, Mechanism and Manipulators
- Energy Systems, Renewable Energy and Fuel Cells
- Engineering Design (Theory and Education)
- Instrumentation, Inspection and Industrial Sensors
- Manufacturing and Production Process
- Marine and Ocean Engineering
- Material Sciences and Engineering
- Mechanics, Dynamics and Finite Element Methods
- Mechanical Engineering Education
- Modeling, Design, Simulation and Optimization
- MEMS and Nano Technologies
- Thermodynamics and Fluid Mechanics
- Vehicle Dynamics, Systems and Powertrains

CONCURRENT CONFERENCES

- Advances and New Trends in Engineering Design
- 22nd Annual Conference of the CFD Society of Canada
- MIE Graduate Research Showcase
- Ontario-on-a-Chip9/MATCH

SPECIAL SYMPOSIUMS

- Advanced Energy Systems
- CCToMM 2014 - Mechanisms, Machines, Mechatronics
- Cell Mechanics and Nanomechanics
- Combustion and Engines
- Droplet dynamics, Thermodynamics and Coatings
- Green Technology and Intelligent Manufacturing
- Manufacturing, Plastics and Polymers
- MEMS and Instrumentation
- Microfluidics
- Multiscale Simulation; Multifunctional Materials and Structures
- Robotics, Dynamics and Autonomous Systems
- Soft Matter
- Advanced Road Vehicles
- Women in Engineering
- For details of the congress please check the home page of the conference: http://www.mie.utoronto.ca/csme2014/index.html.

The Engineering Institute of Canada Honours, Awards and Fellowships

The Engineering Institute of Canada is pleased to announce the 2014 recipients of its honours, awards and fellowships.

The senior awards of EIC are the highest distinctions made by the Institute and are awarded to members of its technical societies. Five senior medals recipients will be presented at the 2014 Awards Gala in recognition of outstanding achievement or service to the engineering profession. 18 engineers become Fellows of EIC for their exceptional contributions to engineering in Canada.

EIC President Jean Zu will present the recipients at the Institute's Annual Awards Banquet at the Westin Hotel in Ottawa on 15 March 2014.

The 2014 senior award recipients from CSME are:

JULIAN C. SMITH MEDAL

Greg F. Naterer, CSME, St. John's, NL

FELLOWS

Nasser Ashgriz, CSME, Toronto, ON; Sushanta Mitra, CSME, Edmonton, AB

The 24th International Congress of Theoretical and Applied Mechanics (ICTAM2016), Montreal, Quebec, Canada, August 21-26, 2016

The 24th International Congress of Theoretical and Applied Mechanics (ICTAM2016) will be held in Montreal, Quebec, Canada, from August 21 to 26, 2016. The National Research Council Canada will host the congress. For detailed information of this congress, please check the webpage at http://www.ictam2016.org/ or contact

Congress Management Office - ICTAM 2016
National Research Council Canada
1200 Montréal Road, Building M-19
Ottawa, ON Canada K1A 0R6
e-Mail: ICTAM2016@nrc-cnrc.gc.ca

Bureau de gestion du congrès - ICTAM 2016
Conseil national de recherches Canada
1200, chemin Montréal, Édifice M-19
Ottawa (Ontario) Canada K1A 0R6
courriel: ICTAM2016@nrc-cnrc.gc.ca

This is the twenty-fourth in a series of quadrennial conferences that began in Delft, The Netherlands in 1924. In 1946, during the sixth congress in Paris, the International Union of Theoretical and Applied Mechanics (IUTAM) was founded. ICTAM congress is the largest gathering of researchers and engineers in the general area of mechanics from the world. It provides an international forum for communicating the most recent advances, sharing findings, refining ideas, and building partnerships.

The most recent ICTAM Congress was the 23rd Congress in Beijing in 2012. The last and the only ICTAM Congress held in Canada is the 15th Congress in 1980 in Toronto.

Please register at http://www.ictam2016.org/ to receive further information about the congress.

ICTAM 2016
MONTRÉAL

24th **International Congress of Theoretical and Applied Mechanics**

24e **Congrès international de mécanique théorique et appliquée**

Palais des congrès, Montréal, Canada
August 21-26 août 2016

Mechanics — Foundation of Multidisciplinary Research

La méchanique — fondement de la recherche multidisciplinaire

Congress Management Office
National Research Council Canada
1200 Montréal Road, Building M-19
Ottawa, ON   Canada K1A 0R6

ICTAM2016@nrc-cnrc.gc.ca

Bureau de gestion du congrès
Conseil national de recherches Canada
1200, chemin Montréal, Édifice M-19
Ottawa (Ontario) Canada K1A 0R6

ICTAM2016@nrc-cnrc.gc.ca

In order to receive future announcements and other information about the Congress, register your interest at :
Si vous désirez obtenir des annonces et toutes informations relatives au congrès, veuillez remplir la déclaration d'intérêt à l'adresse suivante :

Photos © NASA and Tourisme Montréal

www.ictam2016.org

UNIVERSITY OF ALBERTA
Department of Mechanical Engineering

UNIVERSITÉ DE MONCTON
Département de génie mécanique

QUEEN'S UNIVERSITY
Department of Mechanical Engineering

UNIVERSITY OF BRITISH COLUMBIA
Department of Mechanical Engineering

UNIVERSITY OF MANITOBA
Department of Mechanical and Industrial Engineering

ROYAL MILITARY COLLEGE OF CANADA
Department of Mechanical Engineering

McGill
Department of Mechanical Engineering

Laurentian University Université Laurentienne
Department of Mechanical Engineering

RYERSON UNIVERSITY
Department of Mechanical Engineering

Carleton UNIVERSITY
Department of Mechanical and Aerospace

McMaster University ENGINEERING
Department of Mechanical Engineering

UNIVERSITÉ DE SHERBROOKE
Département de génie mécanique

Concordia UNIVERSITY
Department of Mechanical Engineering

Memorial University of Newfoundland
Department of Mechanical Engineering

WESTERN ENGINEERING The University of Western Ontario
Department of Mechanical Engineering

DALHOUSIE (DAL TECH)
Department of Mechanical Engineering

UNIVERSITY OF OTTAWA / UNIVERSITÉ D'OTTAWA
Department of Mechanical Engineering / Département de génie mécanique

UNIVERSITY OF VICTORIA
Department of Mechanical Engineering

UNIVERSITY OF SASKATCHEWAN
Department of Mechanical Engineering

UNIVERSITY OF NEW BRUNSWICK
Department of Mechanical Engineering

ÉCOLE POLYTECHNIQUE MONTRÉAL

UNIVERSITY OF WATERLOO
Department of Mechanical Engineering

UNIVERSITY OF ONTARIO INSTITUTE OF TECHNOLOGY
Faculty of Engineering and Applied Science

UNIVERSITY OF TORONTO
Department of Mechanical and Industrial Engineering

UNIVERSITY OF WINDSOR
Department of Mechanical Engineering

Lakehead UNIVERSITY
Department of Mechanical Engineering

UNIVERSITÉ LAVAL
Faculté de sciences et de génie
Département de génie mécanique